ARTICLE IN PRESS

Transplantation and Cellular Therapy 000 (2026) 1–14

Transplantation and Cellular Therapy

journal homepage: www.astctjournal.org

Biomarkers

Proteomic Signatures and Early Biomarkers Predicting Veno-Occlusive Disease in Pediatric Patients Undergoing Haploidentical Hematopoietic Cell Transplantation with Busulfan-Based Conditioning and Post-Transplant Cyclophosphamide

Kyung Taek Hong[1,2,†], Suwan Yu[3,†], Jin Woo Jung[4,5], Yooeun Kim[3], Jung Yoon Choi[1,2], Sang Hoon Song[7], Kwangsoo Kim[5,6], Dohyun Han[4,5,6,#], Hyoung Jin Kang[1,2,8,#,*]

[1] *Department of Pediatrics, Seoul National University College of Medicine, Seoul National University Children's Hospital, Seoul, Republic of Korea*
[2] *Seoul National University Cancer Research Institute, Seoul, Republic of Korea*
[3] *Interdisciplinary Program in Bioinformatics, College of Natural Sciences, Seoul National University, Seoul, Republic of Korea*
[4] *Proteomics Core Facility, Biomedical Research Institute, Seoul National University Hospital, Seoul, Republic of Korea*
[5] *Department of Transdisciplinary Medicine, Institute of Convergence Medicine with Innovative Technology, Seoul National University Hospital, Seoul, Republic of Korea*
[6] *Department of Medicine, College of Medicine, Seoul National University, Seoul, Republic of Korea*
[7] *Department of Laboratory Medicine, Seoul National University College of Medicine, Seoul, Republic of Korea*
[8] *Wide River Institute of Immunology, Hongcheon, Republic of Korea*

Article history:
Received 11 July 2025
Accepted 16 December 2025

Key Words:
Plasma proteomics
Biomarker discovery
VOD (veno-occlusive disease)
HSCT (hematopoietic stem cell transplantation)
Busulfan conditioning
Pediatrics

A B S T R A C T

Hepatic veno-occlusive disease (VOD), or sinusoidal obstruction syndrome, is a life-threatening complication following hematopoietic cell transplantation (HSCT). In pediatric patients, busulfan-based myeloablative conditioning is a major risk factor. This study aimed to identify plasma proteomic biomarkers predictive of VOD development in children undergoing haploidentical HSCT with busulfan-based conditioning and post-transplant cyclophosphamide (PTCy). Plasma samples were collected from 51 children (VOD, n = 26; control, n = 25) at baseline and 1 to 4 h postbusulfan infusion on days −8 to −5. Proteomic profiles using liquid chromatography-tandem mass spectrometry identified 720 proteins. Differential abundance, longitudinal clustering, pathway enrichment, and machine learning-based biomarker selection were performed. The VOD group exhibited predominantly down-regulated proteins, with minimal changes from baseline during early treatment. Pathway enrichment analysis revealed distinct temporal patterns between the groups. At baseline, the VOD group showed enrichment in homeostasis-related pathways, while

Financial disclosure: See Acknowledgments on page XXX.

*Correspondence and reprint requests: Hyoung Jin Kang, MD, PhD, Department of Pediatrics, Seoul National University College of Medicine, Seoul National University Cancer Research Institute, 101 Daehak-ro, Jongno-gu, Seoul 03080, Republic of Korea.

E-mail addresses: hdh03@snu.ac.kr (D. Han), kanghj@snu.ac.kr (H.J. Kang).

† These authors have contributed equally to this manuscript.

# These are corresponding authors equally contributed to the manuscript.

https://doi.org/10.1016/j.jtct.2025.12.989

detoxification pathways were persistently activated postconditioning. In contrast, the control group demonstrated early activation of detoxification pathways, which gradually declined, suggesting effective oxidative stress management. A machine learning model, trained on a discovery cohort (70%) and 30% validated on a separate cohort (30%), identified 15 biomarkers. Notably, glutamate-cysteine ligase catalytic subunit (GCLC), crucial for glutathione biosynthesis, and fructose-bisphosphatase 1 (FBP1), a gluconeogenic enzyme, were down-regulated at baseline in the VOD group. Baseline down-regulation of proteins such as GCLC and FBP1 may serve as early biomarkers for predicting VOD, facilitating timely prophylactic interventions in high-risk pediatric patients undergoing haploidentical HSCT with busulfan-based conditioning and PTCy.

INTRODUCTION

Hepatic veno-occlusive disease (VOD), also known as sinusoidal obstruction syndrome, is a life-threatening complication following hematopoietic cell transplantation (HSCT). Its pathophysiology involves endothelial cell injury and detachment induced by factors such as high-dose chemotherapy, leading to sinusoidal obstruction and postsinusoidal portal hypertension [1]. Pediatric VOD incidence ranges from 15% to 30%, varying according to age, underlying disease, and conditioning regimens [2,3]. Severe VOD occurs in 30% to 40% of cases, with mortality rates reaching up to 80% [4,5].

In pediatric patients, busulfan-based myeloablative conditioning is a significant risk factor for hepatic VOD [6]. The use of post-transplant cyclophosphamide (PTCy), which facilitates broader application of haploidentical donors, has raised concerns regarding increased risk of VOD when combined with myeloablative conditioning regimens [7–9]. The recent European Society for Blood and Marrow Transplantation (EBMT) criteria have improved diagnostic sensitivity, enabling earlier detection of VOD [10,11]. Preventive or early treatment with defibrotide has been shown to reduce morbidity and improve outcomes in the pediatric population [2,3,10]. Thus, predefined risk factors for hepatic VOD should be carefully evaluated before HSCT to ensure timely prophylactic interventions and optimize outcomes in pediatric HSCT patients.

Plasma protein biomarkers for diagnosing or predicting the severity of hepatic VOD have been investigated in adult and pediatric patients undergoing HSCT across various studies. Biomarkers such as hyaluronic acid, L-Ficolin, vascular cell adhesion molecule-1, intercellular adhesion molecule-1, and angiopoietin-2 have been proposed as useful diagnostic and prognostic indicators [12,13]. However, these biomarkers have primarily been evaluated starting from the day of HSCT. No previous studies have explored serial plasma proteomics before and during busulfan-based myeloablative conditioning.

This study utilized prospectively collected plasma samples from a pediatric cohort undergoing haploidentical HSCT with busulfan-based myeloablative conditioning and PTCy to identify proteomic biomarkers predictive of VOD development. By comparing plasma proteomic profiles between severe VOD cases and controls, the study aimed to discover early biomarkers for VOD detection and to investigate dynamic proteomic changes during busulfan conditioning. Our objective was to characterize key proteomic signatures associated with VOD risk, thereby enhancing understanding of its pathophysiology and providing potential strategies for early intervention.

MATERIALS AND METHODS

Clinical Cohorts

In this study, 51 pediatric patients who underwent haploidentical HSCT with busulfan-based myeloablative conditioning and PTCy at Seoul National University Children's Hospital between 2015 and 2021 were enrolled. Patients were divided into two groups: 26 patients diagnosed with severe or very severe hepatic VOD post-HSCT (VOD group) and 25 age- and diagnosis-matched patients who did not develop VOD (control group). The European Society for Blood and Marrow Transplantation (EBMT) diagnostic and severity criteria for VOD were used in this study [11]. All patients received a conditioning regimen comprising targeted busulfan, fludarabine, and cyclophosphamide, as previously described [9]. Graft-versus-host disease prophylaxis consisted of PTCy (50 mg/kg i.v. once daily on days +3 and +4), tacrolimus, and mycophenolate mofetil (Figure 1A). Mobilized peripheral blood was used as the stem cell source, and prophylaxis for VOD included lipoprostaglandin E1 and/or ursodeoxycholic acid. Plasma samples were collected at five time points, starting with a baseline sample prior to busulfan administration and 1 to 4 h postinfusion from day −8 to −5. The study was approved by the Institutional Review Board, and informed consent was obtained from the legal guardians.

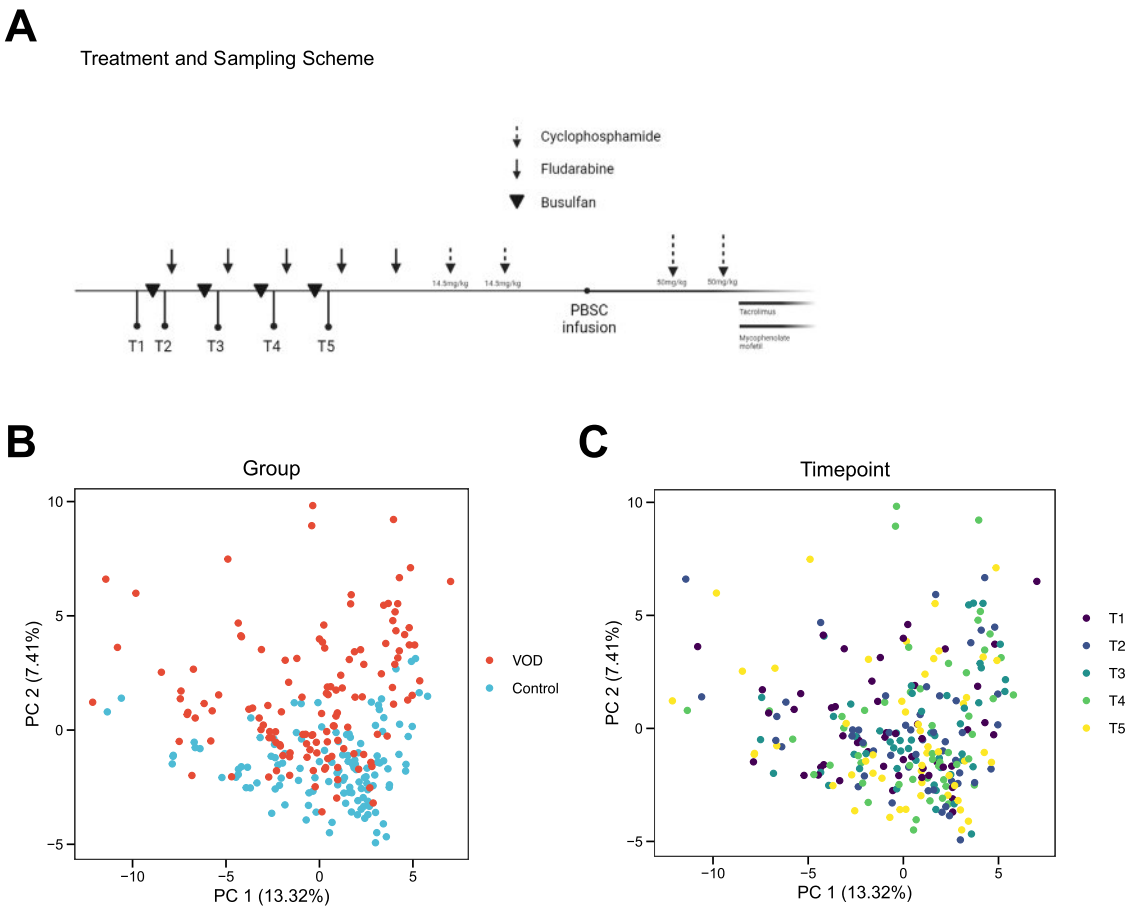

Figure 1. Study design and PCA analysis. (A) Treatment and sampling scheme. Lines with circles indicate time points (T1 to T5) for sample collection during the treatment process. Arrows indicate the timing of cyclophosphamide (↓), fludarabine (↓), and busulfan (▼) administration. (B) PCA plots illustrating sample distribution between VOD and control groups. (C) PCA plot demonstrating the distribution of samples across the five time points (T1 to T5).

Sample Preparation

Plasma samples (30 μL) were diluted 1:4 in multiple affinity removal system buffer A (Agilent Technologies, Santa Clara, CA) and filtered with 0.22 μm Spin-X filters (Corning Costar, NY) to remove six high-abundance proteins (albumin, immunoglobulin [Ig] G, IgA, transferrin, haptoglobin, and antitrypsin). Individual plasma samples were depleted using a multiple affinity removal system column (Hu-6HC, 4.6 × 100 mm, Agilent Technologies) on an Agilent 1260 HPLC system. Depleted plasma samples were concentrated using a 3 kDa Amicon filter (Millipore, Burlington, MA), and protein concentrations were determined via the bicinchoninic acid assay.

For protein digestion, 100 μg of each sample was precipitated by adding a fivefold volume of ice-cold acetone. Dried samples were reconstituted in 50 μL SDT buffer (2% sodium dodecyl sulphate, 0.1 M dithiothreitol in 0.1 M Tris HCl pH, 8.0), heated at 95°C, and digested using a filter-aided sample preparation method, as previously described with some modifications [14,15]. Briefly, proteins were loaded onto a 30 kDa Amicon filter (Millipore, Billerica, MA), and the buffer was exchanged with UA solution (8 M urea in 0.1 M Tris-HCl pH, 8.5) via centrifugation. After three buffer exchanges with UA solution, the reduced cysteines were alkylated with 0.05 M iodoacetamide in UA solution for 30 min in the dark at room temperature. The UA buffer was exchanged twice with 40 mM ammonium bicarbonate. Protein samples were digested with trypsin/LysC (enzyme to substrate ratio of 1:100) at 37°C overnight. The resulting peptides were collected in new Eppendorf tubes via centrifugation, and an additional elution step was performed using 40 mM ammonium bicarbonate and 0.5 M NaCl. All resulting peptides were acidified with 10% trifluoroacetic acid and desalted using in-house C18-StageTips, as described previously [14]. The desalted peptides were completely dried in a vacuum dryer and stored at −80°C.

Data-Independent Acquisition (DIA)—Mass Spectrometry (MS) Analysis

Liquid chromatography with tandem MS (LC-MS/MS) analysis was performed using quadrupole Orbitrap mass spectrometers, Q-Exactive Plus (Thermo Fisher Scientific, Waltham, MA), coupled to an Ultimate 3000 RSLC system (Dionex, Sunnyvale, CA) with a nano-electrospray source as previously described, with some modifications [16]. Peptide samples were separated on a two-column setup with a trap column (300 μm I. D. × 5 mm, C18 3 μm, 100 Å) and an analytical column (75 μm I.D. × 50 cm, C18 1.9 μm, 100 Å). Prior to sample injection, the dried peptide samples were re-dissolved in solvent A (2% acetonitrile and 0.1% formic acid). After the samples were loaded onto the nano LC,

a 120-min gradient from 8% to 30% solvent B (100% acetonitrile and 0.1% formic acid) was applied to all samples. The spray voltage was 2.0 kV in positive ion mode, and the temperature of the heated capillary was set to 320°C. The DIA method consisted of a survey scan at 70,000 resolution from 400 to 1220 m/z (AGC target of 3 × 106 or 60-ms injection time). Further, 19 DIA variable windows were acquired at a resolution of 35,000 with an automatic gain control target of 3e6 and auto injection time [16]. The stepped collision energy was 10% at 27%.

Proteomic Data Processing

To generate spectral libraries, 24 data-dependent acquisition measurements were performed on the pooled samples. Hybrid library was generated from data-dependent acquisition and individual DIA run files using Spectronaut implements database search engine, Pulsar, against the UniProt Human Database (July 2021, 101,014 entries) and the indexed retention time standard peptide sequence. DIA data from individual samples were analyzed using Spectronaut 15 (Biognosys, Schlieren-Zurich, Switzerland). First, the DIA raw files were converted into HTRMS format using the GTRMS converter tool provided by Spectronaut. The false discovery rate was estimated using the mProphet [17] approach and set to 1% at the peptide precursor and protein levels. The proteins were inferred by the software, and the quantification information was acquired at the protein level using a q-value <0.01 criterion. This q-value threshold pertains to ID/quantification QC only and is distinct from the subsequent analysis.

Statistical and Bioinformatics Analysis

LC-MS/MS quantified 720 proteins across all plasma samples after quality control. Quantile normalization was applied to standardize protein abundances between samples. Protein IDs were mapped to gene symbols using the differentially expressed protein (DEP) R package (version 1.26.0). Principal component analysis (PCA) was conducted on the top 100 most variable proteins to evaluate the distinct proteomic distribution between the VOD and control groups.

Differential abundance between VOD and control was tested separately at each time point (T1 to T5) using the Wilcoxon rank-sum test; proteins were considered DEPs abundant if $P < .05$ and $|\log2FC| > 0.25$. Results were visualized using volcano plots (ggVolcano R package, version 0.0.2) and heatmaps (ComplexHeatmap R package, version 2.20.0), displaying median fold-change differences between groups over time.

Longitudinal clustering analysis identified proteins with significant temporal abundance changes using Friedman's test ($P < .05$). For these selected proteins, mean protein expression was calculated for each group, followed by z-score normalization across time points. Fuzzy c-means clustering was conducted using the Mfuzz R package (version 2.64.0), with the number of clusters set to five. This clustering approach allowed for the identifying distinct temporal proteomic patterns across the treatment timeline.

To identify enriched biological pathways and disease-specific associations involved in VOD pathogenesis, we performed pathway enrichment and protein–protein interaction (PPI) analyses. The clusterProfiler R package (version 4.12.6) was used for over-representation pathway analysis, leveraging databases such as GO (BP, MF, CC), KEGG, and DiGeNet. Significantly enriched pathways were identified using a P value threshold of <.05. For directionality, over-representation pathway analysis was run separately on up- and down-regulated DEP lists at baseline, and results are displayed as a signed $-\log10(P)$ (positive for up-regulated lists; negative for down-regulated lists, VOD versus control). PPI analysis was constructed with STRING (version 12.0), applying a confidence score threshold of 0.4.

Machine Learning-Based Biomarker Selection

In this study, machine learning-based feature selection was utilized to identify baseline biomarkers predictive of VOD before busulfan conditioning and to develop a predictive model across multiple time points. The cohort was split into a discovery set (70%) and a validation set (30%) using stratified sampling to ensure a balanced distribution of VOD cases and controls. DEPs at time point T1 were prioritized based on P values obtained from the Wilcoxon rank-sum test. Recursive feature addition with cross-validation (RFA-CV) was employed to identify the optimal biomarker set. Features were iteratively added, starting from the highest-ranked, to maximize fivefold CV accuracy on the discovery cohort using T1 proteomics data. Features were added sequentially until all 102 DEPs from T1 were included. Model performance was estimated through fivefold CV, where subsets of the discovery data were used for training and the remainder for validation.

To minimize model-specific biases, multiple machine learning algorithms were tested, including AdaBoost, decision trees, extra trees (ET), gradient boosting, logistic regression (LR), random forest, and support vector machines. These models were trained on the discovery cohort using selected biomarkers from T1 proteomics data, with performance evaluated on the holdout validation cohort. Model selection was primarily based on accuracy achieved in the validation cohort at T1. To assess the model's generalizability across multiple time points, the final model trained on T1 data was also applied to time points T2 to T5 in the validation cohort.

Survival Analysis

Kaplan–Meier survival analysis was performed to compare overall survival (OS) and event-free survival (EFS) between the VOD and control groups. OS was defined as the time from HSCT until death from any cause, while EFS was defined as the time from HSCT until disease progression, relapse, or death. Survival was evaluated using the Kaplan–Meier method, and differences in survival rates were assessed using the log-rank test. Statistical significance was set at $P < .05$. Statistical analyses were conducted using SPSS version 23.0 (IBM, Armonk, NY).

RESULTS

We compared the clinical characteristics of the VOD and control groups. Baseline clinical characteristics, including median age, body weight, and disease type, showed no significant differences (Table 1). For instance, the median age was 8.5 yr in the VOD group compared to 6.5 yr in the control group ($P = 0.391$), and the majority of patients in both groups had malignant diseases (88.5% in VOD versus 88.0% in control; $P = .959$). None of the patients in either group had received gemtuzumab or inotuzumab prior to HSCT, nor had they experienced recent hepatic infections. There were no

Table 1
Patient's Characteristics According to the Groups

Variables	VOD Group (n = 26)	Control Group (n = 25)	P Value
Median age, yr (range)	8.5 (1.3-18.8)	6.5 (0.9-15.9)	.391
Gender, n			.683
Male	15 (57.7%)	13 (52.0%)	
Female	11 (42.3%)	12 (48.0%)	
BSA, m^2 (range)	1.1 (0.5-1.8)	0.9 (0.5-1.7)	.295
Body weight, kg (range)	30.2 (10.6-73.0)	25.9 (10.4-57.7)	.268
Height, cm (range)	133.6 (83.6-167.7)	127.6 (76.1-178.0)	.386
Disease, n			.959
Malignancy	23 (88.5%)	22 (88.0%)	
Non-malignant ds	3 (11.5%)	3 (12.0%)	
CMV sero-status, n			.705
Donor+/Recipient+	22 (84.6%)	19 (76.0%)	
Donor+/Recipient−	3 (11.5%)	5 (20.0%)	
Donor−/Recipient+	1 (3.8%)	1 (4.0%)	
Busulfan AUC (mg × h/L)			
Day 1	19.4 (12.1-29.1)	21.4 (12.8-32.4)	.192
Day 2	19.8 (13.6-27.2)	19.4 (12.4-25.6)	.461
Day 3	20.5 (14.5-28.1)	19.4 (15.0-32.9)	.596
Day 4	15.7 (3.3-29.3)	12.7 (1.4-23.3)	.392
Total	74.7 (72.1-81.4)	74.1 (72.6-77.2)	.13
Pre-HSCT ferritin (ng/mL)	1158 (25-8412)	802 (6-18,261)	.828
Peak AST/ALT within 1 mo before HSCT (CTCAE grade)			.451
Grade 0	14 (53.8%)	10 (40.0%)	
Grade 1	8 (30.8%)	12 (48.0%)	
Grade 2	4 (15.4%)	3 (12.0%)	
Peak total bilirubin within 1 mo before HSCT (CTCAE grade)			.413
Grade 0	22 (84.6%)	23 (92.0%)	
Grade 1	4 (15.4%)	2 (8.0%)	
HSCT Comorbidity Index			.773
0	14 (53.8%)	15 (60.0%)	
1-2	7 (26.9%)	7 (28.0%)	
≥3	5 (19.2%)	3 (12.0%)	
Acute GVHD, n			.771
Yes	9 (36.0%)	10 (40.0%)	
No	16 (64.0%)	15 (60.0%)	
Chronic GVHD, n			.938
Yes	3 (15.8%)	4 (16.7%)	
No	16 (84.2%)	20 (83.3%)	
Event, n			.406
Yes	9 (34.6%)	6 (24.0%)	
No	17 (65.4%)	19 (76.0%)	
Survival, n			.057
Alive	17 (65.4%)	22 (88.0%)	
Death	9 (34.6%)	3 (12.0%)	
Median follow-up time, yr (range)	3.6 (0.1-8.6)	6.4 (0.7-8.6)	.002

ALT indicates alanine aminotransferase; AST, aspartate aminotransferase; AUC, area under the curve; BSA, body surface area; CMV, cytomegalovirus; CTCAE, common terminology criteria for adverse events; GVHD, graft-versus-host disease; HSCT, hematopoietic stem cell transplantation; n, number; VOD, veno-occlusive disease.

differences between the groups in the peak levels of alanine aminotransferase, aspartate aminotransferase, total bilirubin within 1 mo before HSCT, or in the HSCT Comorbidity Index [18]. There were no thrombotic microangiopathy events in the entire cohort, except for one patient in the VOD group, whose condition improved spontaneously without eculizumab treatment.

All patients in the VOD group developed either severe (n = 16) or very severe VOD (n = 10). The defining criteria for severe VOD included elevated total bilirubin (n = 6), impaired coagulation (n = 5), persistent refractory thrombocytopenia (n = 4), and abnormal liver function test results (n = 1). The criterion for very severe VOD was renal failure requiring renal replacement therapy in all affected patients. The median onset of VOD was 17 days post-HSCT (range, 5 to 37 days). Only four cases occurred after day 21 post-HSCT (on days 25, 25, 29, and 37). Survival analysis demonstrated significantly reduced OS in the VOD group compared to the control group (P = .043), indicating that the development of VOD adversely impacted OS outcomes (Supplementary Figure S1A). The causes of death in the VOD group were disease-related (n = 4), infection with respiratory failure (n = 3), and VOD-related multiorgan failure (n = 2), whereas those in the control group were disease-related (n = 2) and infection (n = 1), respectively. However, there was no significant difference in EFS between the groups (P = .301).

Distinct Proteomic Profiles in VOD and Control Patients Following HSCT with Busulfan-Based Conditioning

Plasma samples were collected at five distinct time points and analyzed using LC/MS-MS (Figure 1A). After preprocessing, a total of 720 proteins were quantified. PCA was conducted to evaluate the overall distribution of proteomic profiles between the VOD and control groups. PCA results demonstrated clear separation between groups, suggesting distinct proteomic profiles (Figure 1B). This separation was consistently observed across all time points, including the preconditioning baseline time point (T1) (Supplementary Figure S1B), indicating significant differences in plasma proteomes between VOD and control patients even prior to the initiation of conditioning therapy. These findings suggest inherent biological differences that may contribute to VOD development. Additionally, the lack of significant clustering based on time alone (Figure 1C) emphasizes that group-specific differences, rather than temporal changes, primarily drive proteomic variations.

Differential Abundance Analysis between VOD and Control Groups Across Pre- and Postconditioning Time Points

To identify differentially abundant proteins between the VOD and control groups across multiple time points, differential abundance analysis was performed. Proteins with an absolute log2 fold-change >0.25 and a P value <.05 (Wilcoxon Rank-Sum test) were considered differentially expressed. At the preconditioning time point (T1), 102 DEPs were identified in the VOD group, of which 64 were down-regulated, and 38 were up-regulated (Figure 2A). At subsequent time points, we identified 103 DEPs at T2 (71 down, 32 up), 106 at T3 (84 down, 22 up), 99 at T4 (65 down, 34 up), and 111 at T5 (62 down, 49 up) (Supplementary Table S1). Pathway analysis of baseline DEPs revealed significant enrichment (P < .05) of biological pathways related to homeostasis and immune system regulation in the VOD group, whereas proteins involved in cell-cell adhesion regulation were significantly downregulated (Figure 2B). This distinct pathway enrichment pattern suggests compensatory mechanisms aimed at maintaining tissue homeostasis in response to underlying biological vulnerabilities. Gene set analysis using the DisGeNET database identified enrichment of proteins associated with various pathological conditions (P < .05), particularly chronic kidney disease, indicating potential pre-existing molecular predispositions in VOD patients (Supplementary Figure 2A). Temporal analysis of protein expression patterns demonstrated that the fold-change values of baseline DEPs remained relatively stable throughout the conditioning period (Figure 2C). This suggests persistent expression differences between the VOD and control groups, independent of busulfan exposure, reflecting inherent biological differences.

We also performed DEP analysis at each postconditioning time point (T2 to T5) to identify consistently expressed proteins. Across these postconditioning time points, a total of 127 proteins were consistently up-regulated, and 112 proteins were consistently down-regulated (Supplementary Table S1). Importantly, none of these DEPs switched expression patterns (from up- to down-regulation or vice versa) during the study period (Supplementary Table S2). This temporal stability was particularly evident among down-regulated proteins, where 34 of 112 down-regulated DEPs exhibited consistently reduced expression across all time points, suggesting persistent suppression throughout conditioning (Supplementary Figure 2B). In contrast, among the total 127 up-regulated DEPs, only

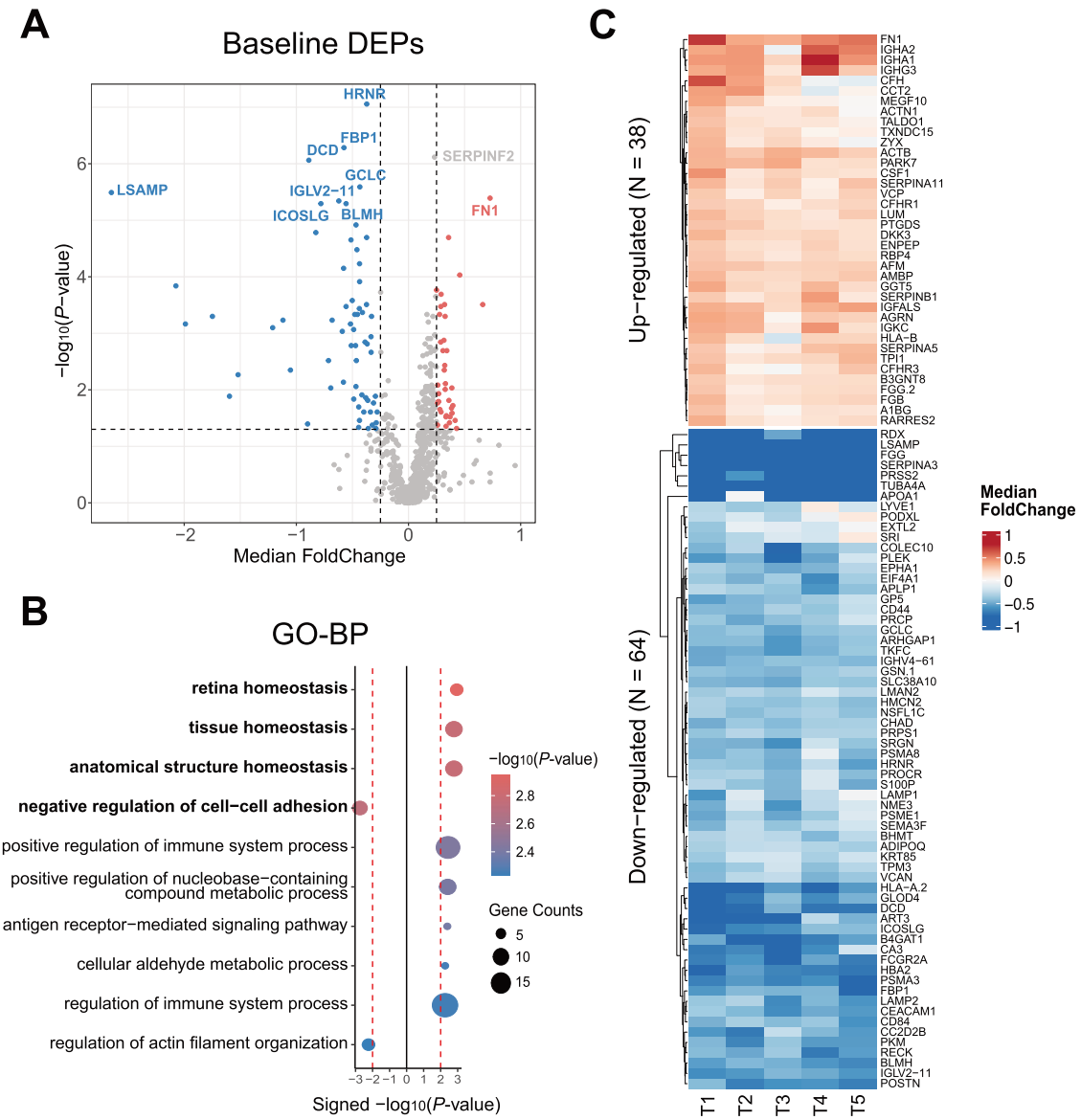

Figure 2. Differential abundance analysis between VOD and control groups. (A) Volcano plots illustrating differential protein abundance between VOD and control groups at each time point (T1 to T5). Colors represent differentially expressed proteins (DEPs) (P value <.05, Wilcoxon rank-sum test) with log fold change (LFC) >0.25. Dashed lines indicate the LFC and P value thresholds. (B) Functional enrichment analysis results showing GO-Biological Process (GO-BP) terms for DEPs ($P < .05$). Circle size indicates gene count, and color intensity represents −log10(P value). Directionality is shown as a signed −log10(P): positive when enrichment is tested on the up-regulated DEP list and negative when tested on the down-regulated DEP list (VOD versus control). Only pathways with P value <.05 are displayed. (C) Heatmap showing the median fold change of up-regulated (UP-DEPs) and down-regulated DEPs (DOWN-DEPs) identified at time point 1 (before conditioning) across 5 time points.

one protein maintained its elevated expression across all time points.

Functional analysis of these down-regulated proteins revealed significant associations ($P < .05$) with biological pathways, including cellular response to insulin stimulus, and molecular functions such as ribonucleotide binding (Supplementary Figure 2C). PPI network analysis identified enrichment of proteins involved in carbon metabolism, including fructose-bisphosphatase 1 (FBP1), PKM, TKFC, and PRPS1 (Supplementary Figure 2D). This persistent differential expression patterns, particularly in down-regulated proteins, suggest that molecular alterations associated with VOD development may originate prior to busulfan conditioning and persist throughout the treatment period.

Dynamic Trajectories of Plasma Proteomic Changes During Busulfan Conditioning

To examine longitudinal plasma proteomic changes in the VOD and control groups, we conducted differential abundance analysis across

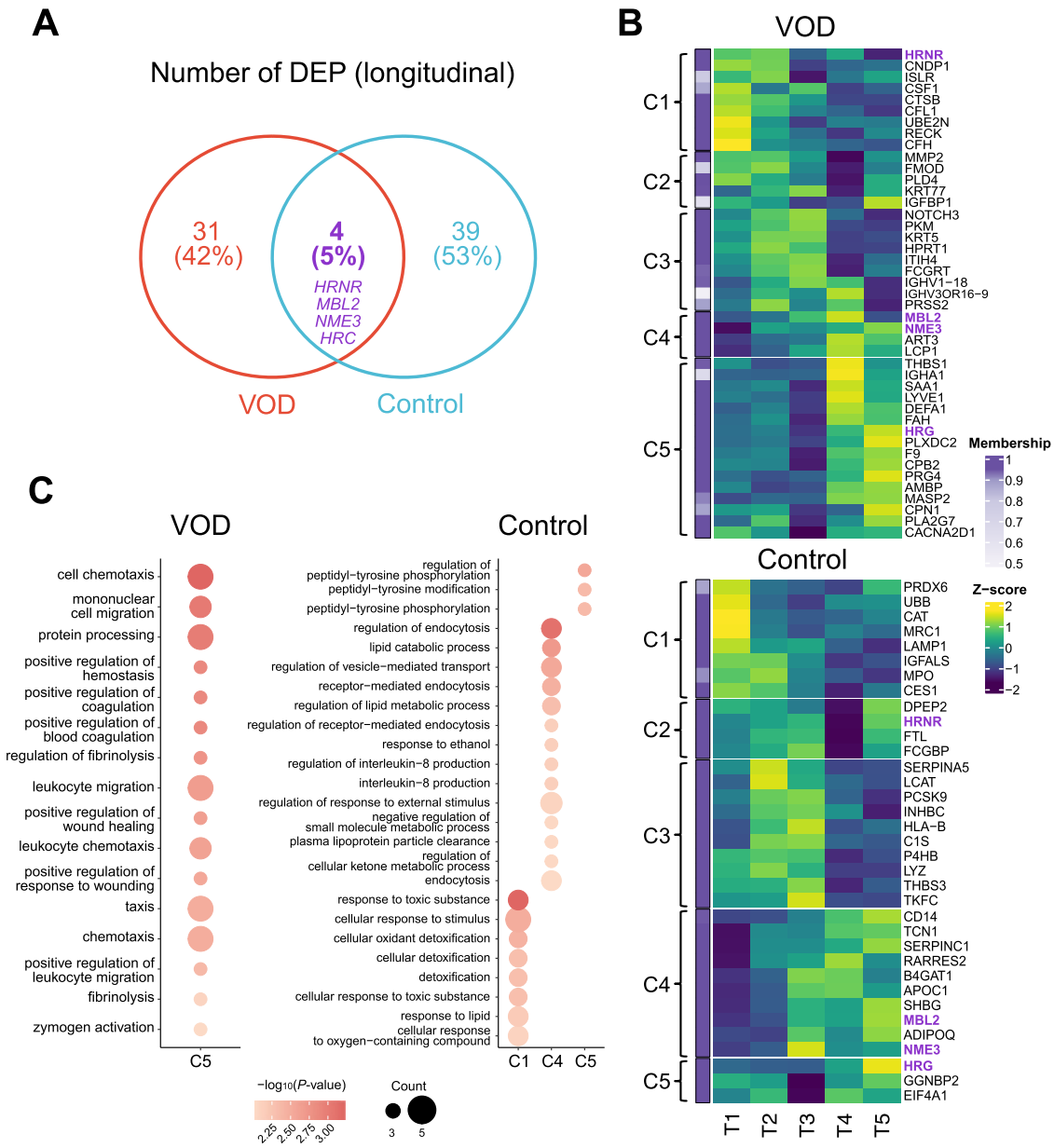

Figure 3. Longitudinal protein expression patterns in VOD and control groups. (A) Venn diagram showing longitudinal differentially abundant proteins in each group. The overlapping region shows proteins that are differentially expressed in both groups over time. (B) Heatmap of longitudinal DEPs with *z*-scaled expression. The left annotation bar shows cluster memberships from part (B) along with membership scores. (C) Functional enrichment analysis of GO-Biological Process (GO-BP) terms for each cluster in VOD (left) and control (right) groups. Circle size is proportional to the number of genes overlapping between the cluster and the GO term, while color intensity indicates statistical significance (−log10(*P* value)). Only pathways meeting the significance threshold ($P < .01$, hypergeometric test) are shown.

multiple time points. This analysis identified 35 temporally dynamic proteins in the VOD group and 43 proteins in the control group (Friedman's test, $P < .05$). The minimal overlap of only four proteins (HRNR, MBL2, NME3, and HRG) between groups (Figure 3A, Fisher's exact test, $P = .1495$) demonstrates that VOD and control groups exhibit independent temporal proteomic responses during treatment, suggesting different molecular adaptation mechanisms in each group.

To further investigate these dynamic expression patterns, clustering analysis was performed on temporally dynamic DEPs. The DEPs were grouped into five clusters, highlighting distinct expression patterns across the five time points (Supplementary Figure 3). Notably, MBL2, NME3, and HRG consistently clustered similarly, showing enrichment at later time points (T4, T5) in both VOD and control groups (Figure 3B). This suggests their expression changes were primarily driven

by busulfan conditioning rather than group-specific factors.

Pathway enrichment analysis of protein clusters revealed notable differences between the VOD and control groups (Figure 3C). In the VOD group, Cluster 5, up-regulated during the later stages, showed enrichment in pathways related to coagulation, fibrinolysis, cell migration, and wound healing ($P < .05$). Conversely, the control group exhibited early enrichment (Cluster 1) of detoxification-related pathways during the initial treatment stages, which declined over time, suggesting more effective mitigation of busulfan-induced oxidative stress. Early activation of these pathways likely enabled the control group to effectively manage oxidative damage, reducing the requirement for sustained activation of damage response mechanisms. In the later treatment stages, the control group demonstrated enrichment in metabolic and phosphorylation-related pathways (Clusters 4 and 5), indicating adaptive cellular mechanisms that promote repair and maintenance of cellular homeostasis in response to controlled oxidative stress and DNA damage induced by busulfan.

Identification of Baseline Biomarkers Predictive of VOD before Busulfan Conditioning

We aimed to identify early biomarkers predictive of VOD development prior to busulfan conditioning (T1) and to construct a machine learning model using these biomarkers. The cohort was randomly divided into a discovery cohort (35 patients, 70%) and a validation cohort (16 patients, 30%). The discovery cohort was used for biomarker selection, while the validation cohort served as in holdout test set to evaluate model performance.

Candidate biomarkers were initially selected based on significant differential expression ($n = 102$, absolute log2 fold-change >0.25, $P < .05$, the Wilcoxon rank-sum test) (Figure 4A). The RFA algorithm was employed to systematically identify the most predictive biomarkers. Starting with the highest-ranked feature, RFA sequentially added features, evaluating performance through fivefold CV to ensure robust feature selection. Multiple machine learning algorithms—including AdaBoost (ADA), decision trees, ET, gradient boosting, LR, random forest, and support vector machines—were assessed to avoid bias and enhance generalizability. Each model determined its optimal biomarker set through RFA, resulting in varied numbers of selected biomarkers (Supplementary Figure 4A,B).

The ET model demonstrated superior performance on the holdout test set, achieving an optimal biomarker set of 15 proteins with an accuracy of 0.938 (Supplementary Figure 4D). Although LR showed slightly higher CV performance (average accuracy = 1.000), the ET model exhibited comparable CV performance (average accuracy = 0.971) with superior generalization capability to unseen data, as indicated by its better performance on the validation cohort (Supplementary Figure 4C,D).

The ET model achieved an AUROC of 0.97 in CV and 1.00 on the test cohort, highlighting its robust predictive accuracy (Figure 4B). Additionally, the model showed high F1-score, specificity, and sensitivity, confirming its effectiveness in predicting VOD risk before busulfan conditioning (F1-score = 0.941, precision = 0.889, recall = 1), confirming its effectiveness in predicting VOD risk prior to busulfan conditioning. These findings indicate that the selected biomarkers and the developed model can accurately predict VOD, potentially aiding in early clinical intervention.

To further evaluate the generalizability of the selected biomarkers, the model was tested across subsequent time points (T2 to T4: during conditioning, T5: postconditioning) (Figure 4C). The model maintained high predictive accuracy at all time points, with AUROC values above 0.961 (range: 0.961 to 1.000), and similarly robust metrics (precision: 0.875 to 1.000, recall: 0.875 to 1.000, accuracy: 0.875 to 1.000, F1-score: 0.875 to 1.000). These results indicate that the selected biomarkers are predictive not only before conditioning but also generalize effectively throughout the treatment course. Notably, the ET model exhibited minimal variation in prediction accuracy over time compared to other models, highlighting its robustness and temporal stability in predicting VOD (Supplementary Figure 4B).

Among the 15 identified biomarkers, two were up-regulated, and 13 were down-regulated at baseline (Figure 5). Except for PSMA8, all biomarkers showed significant quantitative differences ($P < .05$) between the VOD and control groups across all time points, reflecting their temporal stability. Among these biomarkers, HRNR exhibited significant longitudinal clustering differences between groups, suggesting its potential involvement in VOD pathogenesis. Additionally, notable proteins included FBP1, a rate-limiting enzyme in gluconeogenesis, and GCLC, a key enzyme in glutathione biosynthesis. Pathway analysis indicated that these biomarkers are enriched in biological processes relevant to VOD pathogenesis, such as

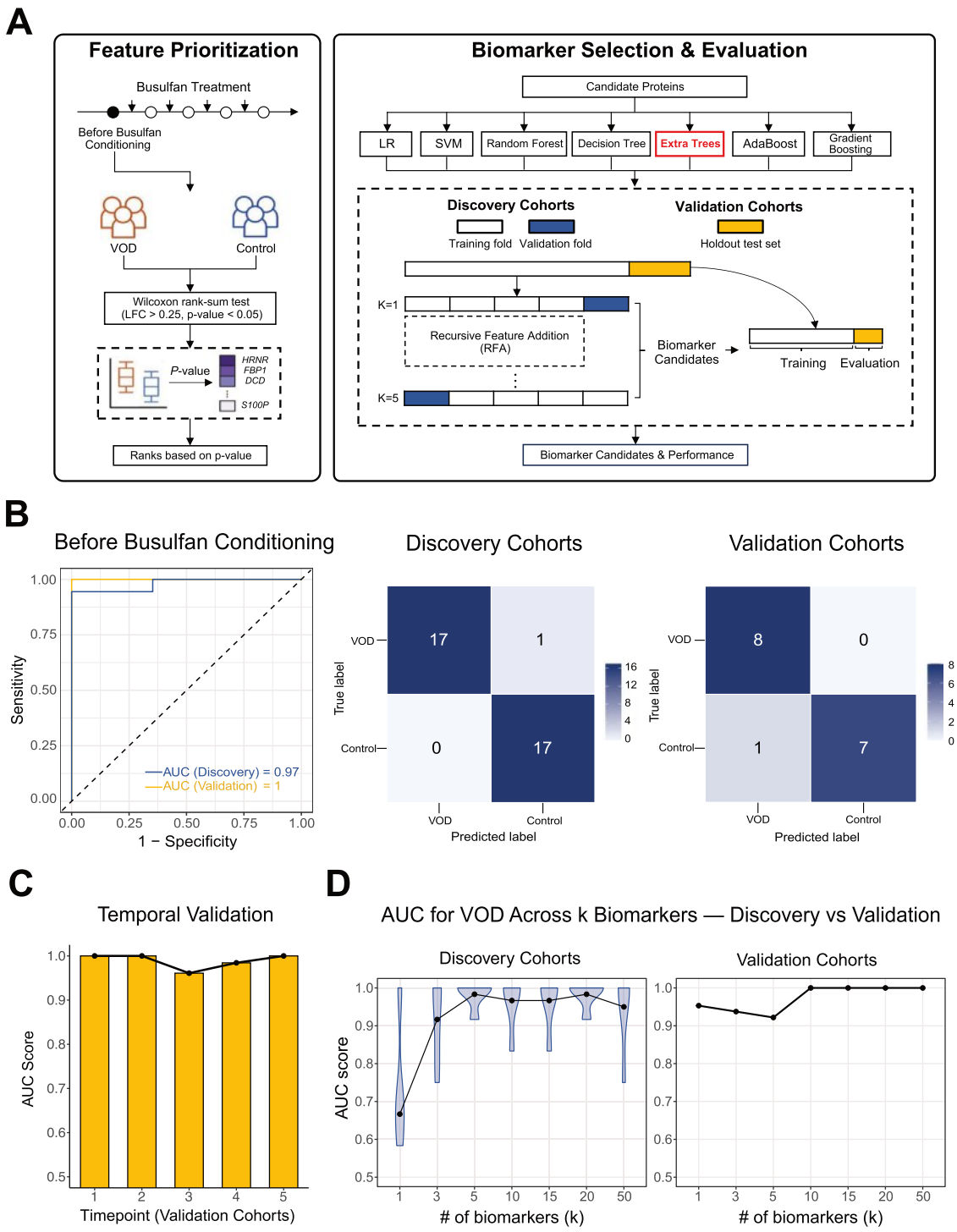

Figure 4. Machine learning-based biomarker discovery for early VOD prediction. (A) Schematic overview of the biomarker discovery pipeline. The workflow consists of two main components: Feature prioritization (left) and biomarker selection and evaluation (right). The initial dataset was stratified into discovery (70%) and validation (30%) sets. Feature prioritization began by selecting baseline (T1) differentially expressed proteins (DEPs) as candidate biomarkers, ranked by Wilcoxon rank-sum test *P* values. The biomarker selection process employed multiple machine learning algorithms, including logistic regression (LR), random forest (RF), support vector machine (SVM), decision tree (DT), extra trees (ET), AdaBoost (ADA), and gradient boosting (GB). Optimal feature selection was performed using recursive feature addition with fivefold cross-validation (RFA-CV). (B) Performance evaluation of the extra trees classifier. Left: Receiver operating characteristic (ROC) curve demonstrating model performance in discovery and validation cohorts. Diagonal dashed line indicates random classification (AUC = 0.5). Right: Confusion matrices for discovery and validation cohorts. (C) Temporal validation of the biomarker-based model. Area under curve (AUC) scores across time points (T1 to T5) in validation cohorts. (D) Model performance according to biomarker panel size. Relationship between the number of selected biomarkers and AUC values in the discovery and validation cohorts.

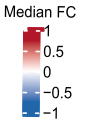

T1	T2	T3	T4	T5	Biomarkers	Protein Class	Key Enriched Pathways
****	*	*	**	***	FN1	extracellular matrix protein	immune system process
****	*		*	*	RARRES2	-	immune system process
****	****	***	****	****	EIF4A1	RNA helicase	-
****	****	****	****	****	GCLC	ligase	sulfur compound metabolic process
****	****	****	***	****	SLC38A10	amino acid transporter	-
****	****	****	***	****	TKFC	cyclase	-
****	***	****		**	PSMA8	protease	protein catabolic process
****	****	****	**	****	HRNR	cytoskeletal protein	-
****	****	**	****	***	BLMH	cysteine protease	sulfur compound metabolic process
****	***	****	***	***	IGLV2–11	immunoglobulin	-
****	****	****	****	****	FBP1	carbohydrate phosphatase	negative regulation of small molecule metabolic process
****	***	**	*	*	ICOSLG	immunoglobulin receptor superfamily	regulation of cell-cell adhesion
****	***	**	****	**	GLOD4	-	-
****	***	**	****	**	DCD	-	-
****	**	**	*	*	LSAMP	immunoglobulin	-

Figure 5. Expression patterns of selected biomarkers. Left: Heatmap showing median fold changes of identified biomarkers over time. Statistical significance indicated as $^{*}P < .05$, $^{**}P < .01$, $^{***}P < .001$, $^{****}P < .0001$. Color scale represents median fold change values. Right: Protein classification and associated enriched pathways of selected biomarkers.

regulation of cell-cell adhesion, immune response, and metabolic processes.

For clinical translation, we examined how AUC scales with biomarker panel size (Figure 4D). The AUC plateaued at approximately five biomarkers—HRNR, FBP1, DCD, GCLC, and LSAMP—with only marginal gains thereafter in both the discovery and validation cohorts (Discovery mean AUC = 0.983, Validation AUC = 0.922). A similar saturation pattern was observed across the other algorithms (Supplementary Figure 4A). These findings suggest that a compact 5-biomarker panel could be sufficient for preconditioning VOD risk stratification, supporting its practical clinical implementation.

DISCUSSION

In this study, we identified baseline and serial dynamic changes in plasma proteomics during busulfan-based myeloablative conditioning in pediatric patients who developed severe hepatic VOD compared to those who did not following HSCT. Although samples originated from retrospective cohorts, all patients shared homogeneous characteristics, including conditioning regimen, GVHD prophylaxis with PTCy, and haploidentical HSCT with peripheral blood stem cells. Previously, we reported a relatively higher incidence of severe VOD in this cohort compared to other HSCT approaches using antithymocyte globulin without PTCy or matched donors [9]. Our findings highlight early plasma proteomic differences associated with the development of hepatic VOD in this specific pediatric population.

We observed more down-regulated DEPs across all time points in the VOD group. Notably, baseline DEPs showed minimal changes during conditioning, suggesting persistent suppression of protective proteomic signatures throughout the busulfan and fludarabine administration period. Interestingly, pathways associated with the cellular response to insulin stimulus were down-regulated in VOD patients. FBP1, a rate-limiting enzyme in gluconeogenesis, was identified as one of the final selected biomarkers in our study. FBP1 deficiency has been linked to steatosis and the senescence of hepatic stellate cells, indicative of deregulated hepatocyte metabolism [19]. This finding suggests the potential of FBP1 as an early predictive biomarker for VOD. Additionally, biological pathway analysis revealed the up-regulation of detoxification pathways in the VOD group, consistent with clustering analysis results. This physiologic response to the conditioning may also serve as an early predictive indicator for VOD.

Functional enrichment analysis using DisGeNET for DEPs at baseline revealed a significant elevation of pathways related to chronic kidney disease in the VOD group. Renal insufficiency is an established risk factor for VOD [20]. Although all patients had normal creatinine levels prior to conditioning, our data suggest a preexisting plasma proteomic signature related to chronic kidney disease in the VOD group, warranting further investigation as a potential predictive marker. However, we did not identify any specific proteins related to renal injury among the final selected biomarkers.

Previous studies demonstrated plasma biomarkers, such as hyaluronan, intercellular adhesion molecule-1, angiopoietin-2, and vascular cell adhesion molecule-1, associated with endothelial cell injury, as relevant to hepatic VOD pathophysiology [1,12,13,21]. However, these biomarkers were evaluated only postconditioning or post-HSCT. Similarly, the Endothelial Activation and Stress Index (EASIX) biomarker panel, which utilizes creatinine, lactate dehydrogenase, and platelet count, are measured on the day of HSCT [22]. These methods have not been able to predict the development of hepatic VOD before the conditioning regimen.

Given the higher VOD incidence in pediatric patients compared to adults [23], prophylaxis prior to conditioning could be beneficial, particularly for high-risk patients. Defibrotide, protecting endothelial cells by reducing procoagulant activity and enhancing fibrinolytic properties, has reduced pediatric hepatic VOD incidence when initiated concurrently with conditioning [3]. Nevertheless, a recent randomized trial reported inefficacy in both pediatric and adult patients [24]. Despite this, prophylactic defibrotide remains promising for pediatric patients at high risk for VOD [2]. Additionally, a higher count of circulating endothelial cells has been proposed as a predictive biomarker for diagnosing VOD and identifying high-risk patients [25]. Circulating endothelial cell counts greater than 17/mL, measured before conditioning, were predictive of VOD development. Consistent with this finding, our study also demonstrates the potential clinical utility of baseline plasma biomarkers, measured prior to conditioning, in predicting severe hepatic VOD and facilitating early defibrotide prophylaxis in high-risk patients.

Longitudinal proteomic analysis during busulfan administration revealed distinct protein profiles between groups, except for four overlapping proteins. Hornerin (HRNR), notably clustered differently between groups (Cluster 1 in VOD, Cluster 2 in control), was among our selected biomarkers (Figure 3B). Hornerin, expressed in epidermal keratinocytes, has also been reported as a potential regulator of tumor vasculature [26]. Notably, the rapid normalization of hornerin levels in the control group compared to the VOD group may indicate its possible protective role following busulfan administration, warranting further research.

Functional enrichment analysis of protein cluster showed distinct biological pathways in each group. The control group demonstrated early detoxification-related pathway activation, declining gradually over time. Conversely, pathways related to coagulation, fibrinolysis, cell migration, and wound healing were upregulated in the VOD group at later time points. These differential adaptive responses likely reflect variations in the management of oxidative damage and endothelial injury. In VOD patients, an inadequate early detoxification response combined with sustained activation of repair mechanisms could contribute to ongoing inflammation and progressive endothelial dysfunction. This contrasts with the more controlled and effective response seen in the control group, where early detoxification and adaptive metabolic pathways appear to mitigate long-term damage.

We identified 15 plasma protein biomarkers for the early prediction of VOD (Figure 5). In addition, when we reduced the number of biomarkers to focus on the most meaningful ones, a panel consisting of five proteins—HRNR, FBP1, DCD, GCLC, and LSAMP—showed a comparable AUC. This comprehensive approach provides robust predictive capability for VOD, enabling timely clinical interventions. Among these biomarkers, glutamate-cysteine ligase catalytic subunit (GCLC), which plays a key role in the first step of glutathione biosynthesis [27], was identified as a significantly downregulated DEP in the VOD group. Given that busulfan is metabolized by liver cytosolic glutathione-S-transferase, reduced hepatic glutathione levels may contribute to hepatic damage and the development of VOD. While glutathione S-transferase M1 polymorphism is a known VOD risk factor [28], decreased plasma levels of GCLC might further impair busulfan metabolism. However, many selected biomarkers lack clear direct associations with VOD pathogenesis, emphasizing the need for validation in larger cohorts. In the future, it would be worthwhile to investigate the genotype correlations associated with these protein biomarkers that showed lower expression levels. Furthermore, applying these findings not only to allogeneic HSCT but also to pediatric and adolescent patients undergoing autologous HSCT could be valuable to determine their significance. Additionally, no patient in our cohort received prophylactic defibrotide. It may therefore be worthwhile for future studies to investigate plasma proteomics in patients receiving prophylactic defibrotide and to compare these findings with respect to VOD incidence. We plan to perform additional proteomic analyses in patients who received defibrotide prophylaxis to determine whether the expression patterns of these biomarkers differ depending on the use of prophylactic therapy.

This study has several limitations. First, plasma proteomics analysis limits insights into tissue-specific changes, particularly liver-related. Tissue proteomics data would enhance comprehensive pathway understanding. Additionally, we only evaluated plasma proteomics only before and during busulfan administration. Although our primary objective was early plasma biomarker identification, comparisons with post-HSCT plasma proteomics and at VOD onset would further elucidate early biomarker utility. Lastly, external validation—including cross-platform/orthogonal assays (eg, targeted MS or immunoassays)—and integration of additional omics data are needed to confirm robustness and clinical transferability.

In conclusion, our study identified baseline down-regulated plasma proteins, including GCLC and FBP1, as potential early biomarkers for VOD development, enabling timely prophylaxis in high-risk pediatric patients. Furthermore, distinct biological pathway enrichments observed during busulfan-based conditioning suggest variations in oxidative damage management and endothelial injury response as potential physiological biomarkers. These results warrant validation in larger external cohorts.

ACKNOWLEDGMENTS

Financial Disclosure: This research was supported by Korean Society of Hematology (No. ICKSH-2022-08) and by grant No. 04-2021-0300 from the SNUH Research Fund.

Conflict of Interest Statement: The authors have no conflicts of interest to disclose.

Authorship Statement: KTH and SY participated in study design, data collection, data analysis, statistical analysis/interpretation, manuscript drafting, and manuscript revisions. JWJ, YK, JYC, SHS, and KK participated in data collection and data analysis. DH and HJK participated in study design, data analysis, and manuscript editing. All authors have read and approved the manuscript.

Ethics Approval and Consent to Participate: This study was approved by the Institutional Review Board of Seoul National University Hospital, and written informed consent was obtained from the legal guardians of all participating patients before any study procedures commenced (IRB numbers: 0911-050-301 and 2106-087-1228).

Availability of Data and Materials: The datasets generated and analyzed during the current study are available from the corresponding author on reasonable request.

SUPPLEMENTARY MATERIALS

Supplementary material associated with this article can be found, in the online version, at doi:10.1016/j.jtct.2025.12.989.

REFERENCES

1. Carreras E, Diaz-Ricart M. The role of the endothelium in the short-term complications of hematopoietic SCT. *Bone Marrow Transplant*. 2011;46(12):1495–1502.
2. Corbacioglu S, Grupp SA, Richardson PG, et al. Prevention of veno-occlusive disease/sinusoidal obstruction syndrome: a never-ending story and no easy answer. *Bone Marrow Transplant*. 2023;58(8):839–841.
3. Corbacioglu S, Cesaro S, Faraci M, et al. Defibrotide for prophylaxis of hepatic veno-occlusive disease in paediatric haemopoietic stem-cell transplantation: an open-label, phase 3, randomised controlled trial. *Lancet (London, England)*. 2012;379(9823):1301–1309.
4. Carreras E, Díaz-Beyá M, Rosiñol L, Martínez C, Fernández-Avilés F, Rovira M. The incidence of veno-occlusive disease following allogeneic hematopoietic stem cell transplantation has diminished and the outcome improved over the last decade. *Biol Blood Marrow Transplant*. 2011;17(11):1713–1720.
5. Coppell JA, Richardson PG, Soiffer R, et al. Hepatic veno-occlusive disease following stem cell transplantation: incidence, clinical course, and outcome. *Biol Blood Marrow Transplant*. 2010;16(2):157–168.
6. Faraci M, Bertaina A, Luksch R, et al. Sinusoidal obstruction syndrome/veno-occlusive disease after autologous or allogeneic hematopoietic stem cell transplantation in children: a retrospective study of the Italian Hematology-Oncology Association-Hematopoietic Stem Cell Transplantation Group. *Biol Blood Marrow Transplant*. 2019;25(2):313–320.
7. Corbacioglu S, Jabbour EJ, Mohty M. Risk factors for development of and progression of hepatic veno-occlusive disease/sinusoidal obstruction syndrome. *Biol Blood Marrow Transplant*. 2019;25(7):1271–1280.
8. Dalle JH, Giralt SA. Hepatic veno-occlusive disease after hematopoietic stem cell transplantation: risk factors and stratification, prophylaxis, and treatment. *Biol Blood Marrow Transplant*. 2016;22(3):400–409.
9. Hong KT, Park HJ, Kim BK, An HY, Choi JY, Kang HJ. Post-transplantation cyclophosphamide-based haploidentical versus matched unrelated donor peripheral blood hematopoietic stem cell transplantation using myeloablative targeted busulfan-based conditioning for pediatric acute leukemia. *Transplant Cell Ther*. 2022;28(4):195.e191–195.e197.
10. Szmit Z, Gorczynska E, Król A, et al. Introduction of new pediatric EBMT criteria for VOD diagnosis: is it time-saving or money-wasting?: Prospective evaluation of pediatric EBMT criteria for VOD. *Bone Marrow Transplant*. 2020;55(11):2138–2146.
11. Corbacioglu S, Carreras E, Ansari M, et al. Diagnosis and severity criteria for sinusoidal obstruction syndrome/veno-occlusive disease in pediatric patients: a new classification from the European society for blood and marrow transplantation. *Bone Marrow Transplant*. 2018;53(2):138–145.
12. Akil A, Zhang Q, Mumaw CL, et al. Biomarkers for diagnosis and prognosis of sinusoidal obstruction syndrome after hematopoietic cell transplantation. *Biol Blood Marrow Transplant*. 2015;21(10):1739–1745.
13. Putta S, Young BA, Levine JE, et al. Prognostic biomarkers for hepatic veno-occlusive disease/sinusoidal

obstruction syndrome in myeloablative allogeneic hematopoietic cell transplantation: results from the Blood and Marrow Transplant Clinical Trials Network 1202 Study. *Transplant Cell Ther*. 2023;29(3). 166.e161-166.e110.
14. Han D, Jin J, Woo J, Min H, Kim Y. Proteomic analysis of mouse astrocytes and their secretome by a combination of FASP and StageTip-based, high pH, reversed-phase fractionation. *Proteomics*. 2014;14(13-14):1604–1609.
15. Kim SI, Hwangbo S, Dan K, et al. Proteomic discovery of plasma protein biomarkers and development of models predicting prognosis of high-grade serous ovarian carcinoma. *Mol Cell Proteomics: MCP*. 2023;22(3):100502.
16. Jeong HY, An HJ, Sung MJ, et al. Proteomic profiling of protein expression changes after 3 months-exercise in ESRD patients on hemodialysis. *BMC Nephrol*. 2023;24(1):102.
17. Reiter L, Rinner O, Picotti P, et al. mProphet: automated data processing and statistical validation for large-scale SRM experiments. *Nat Methods*. 2011;8(5):430–435.
18. Smith AR, Majhail NS, MacMillan ML, et al. Hematopoietic cell transplantation comorbidity index predicts transplantation outcomes in pediatric patients. *Blood*. 2011;117(9):2728–2734.
19. Li F, Huangyang P, Burrows M, et al. FBP1 loss disrupts liver metabolism and promotes tumorigenesis through a hepatic stellate cell senescence secretome. *Nat Cell Biol*. 2020;22(6):728–739.
20. Roeker LE, Kim HT, Glotzbecker B, et al. Early clinical predictors of hepatic veno-occlusive disease/sinusoidal obstruction syndrome after myeloablative stem cell transplantation. *Biol Blood Marrow Transplant*. 2019;25(1):137–144.
21. Cutler C, Kim HT, Ayanian S, et al. Prediction of veno-occlusive disease using biomarkers of endothelial injury. *Biol Blood Marrow Transplant*. 2010;16(8):1180–1185.
22. Jiang S, Penack O, Terzer T, et al. Predicting sinusoidal obstruction syndrome after allogeneic stem cell transplantation with the EASIX biomarker panel. *Haematologica*. 2021;106(2):446–453.
23. Corbacioglu S, Richardson PG. Defibrotide for children and adults with hepatic veno-occlusive disease post hematopoietic cell transplantation. *Expert Rev Gastroenterol Hepatol*. 2017;11(10):885–898.
24. Grupp SA, Corbacioglu S, Kang HJ, et al. Defibrotide plus best standard of care compared with best standard of care alone for the prevention of sinusoidal obstruction syndrome (HARMONY): a randomised, multicentre, phase 3 trial. *Lancet Haematol*.. 2023;10(5):e333–e345.
25. Farina M, Scaini MC, Facchinetti A, et al. Evaluation of circulating endothelial cells as direct marker of endothelial damage in allo-transplant recipients at high risk of hepatic veno-occlusive disease/sinusoidal obstruction syndrome. *Transplant Cell Ther*. 2024;30(6). 580.e581-580.e514.
26. Gutknecht MF, Seaman ME, Ning B, et al. Identification of the S100 fused-type protein hornerin as a regulator of tumor vascularity. *Nat Commun*. 2017;8(1):552.
27. Ortega AL, Mena S, Estrela JM. Glutathione in cancer cell death. *Cancers*. 2011;3(1):1285–1310.
28. Srivastava A, Poonkuzhali B, Shaji RV, et al. Glutathione S-transferase M1 polymorphism: a risk factor for hepatic venoocclusive disease in bone marrow transplantation. *Blood*. 2004;104(5):1574–1577.